Study of cytotoxicity performance of carbon nanohorns by method of spin probes

Mykola Kartel, Leonid Volodymyr Ivanov, Nikolay A. Lyapunov, Yana O. Cherkashina, Emmanuel Flahaut, Olga A. Gurova, Alexander Vladimirovich Okotrub

https://doi.org/10.1080/1536383X.2020.1757656

Study of cytotoxicity performance of carbon nanohorns by method of spin probes

N. T. Kartel[a], L. V. Ivanov[a], A. N. Lyapunov[b], Y. O. Cherkashina[c], E. Flahaut[d], O. A. Gurova[e], and A. V. Okotrub[e]

[a]Chuiko Institute of Surface Chemistry, NAS of Ukraine, Kiev, Ukraine; [b]Institute for Single Crystals, NAS of Ukraine, Kharkov, Ukraine; [c]Institute for Problems of Cryobiology and Cryomedicine, NAS of Ukraine, Kharkov, Ukraine; [d]University Paul Sabatier, University Toulouse, CIRIMAT, CNRS, INPT, Toulouse 9, France; [e]Nikolaev Institute of Inorganic Chemistry, SB RAS, Novosibirsk, Russia

ABSTRACT

The effects of as-produced and treated by HNO_3(3M) carbon nanohorns on the microviscosity of rat erythrocyte membranes and the viscosity of the water-containing plasma protein matrix were investigated by the method of spin probes. Addition of nanohorns at the concentration of 100 µg/ml to a suspension of erythrocytes led to an increase in membrane microviscosity during 4 h (about 60% effect). In addition, it was shown that nanohorns also induced an increased polarity of the microenvironment for lipophilic probes in the outer layer of membrane phospholipids, as well as disorders in erythrocytes membranes. Addition of nanohorns to plasma led to a little decrease in the viscosity of water and protein matrix, apparently, due to its partial destruction, impacting especially albumin. Pristine and treated by HNO_3(3M) acid nanohorns was found more cytotoxic than nanoparticles of oxidized graphene, and significantly less than carbon nanotubes, which are known to dramatically increase the microviscosity of the membranes of erythrocytes and disrupt their integrity.

KEYWORDS

Carbon nanohorns; cytotoxicity; erythrocyte membranes; the method of spin probes; serum albumin

1. Introduction

Carbon nanomaterials are of particular interest in the field of scientific research and in industrial applications. One of the areas of research and application of carbon nanomaterials is biomedicine.[1,2] Carbon-based nanostructures are not rejected by living tissues and can be used as drug delivery and imaging agents. However, the use of such materials requires an assessment of health risks and an assessment of the environmental impact of nanomaterials.[2,3] One of the first studied carbon nanostructures for medical applications was the molecule C_{60}. Injection of C_{60} into a living organism does not exert a toxic effect, which was observed in the vital activity of animals.[3–6] However, it has also been shown that C_{60} molecules can accumulate in the liver and spleen.

Unlike the fullerene molecule, the discovery of carbon nanotubes (CNTs) introduced a controversial view of their toxicity. Their interaction with the cell and the effect on the living organism as a whole may depend on such parameters as the state of the aggregates, the production method, aspect ratio, cleaning and functionalization of the surface.[7] Of the various types of CNTs, the toxicity of single-wall carbon nanohorns (CNHs) is not clear.

CNHs were first discovered by Iijima and coworkers.[8,9] CNHs are carbon nanostructures belonging to the family of CNTs. They consist of single layers of a graphene sheet wrapped in a tubule with conical caps, a diameter of 2–4 nm, tubule length of 40 to 50 nm and cone angle of 20°.[8,9]

CNHs form spherical aggregates with a diameter of 80–100 nm, inside which there are randomly oriented horn-like layers of graphene about 10 nm in size and a distance between planes about 4–5 nm.[10–12] In general, CNHs are interacting very strongly in these aggregates and it is thus very difficult to separate them into individual nanoparticles. Covalent modification of CNHs modifies their solubility, both in organic solvents and aqueous media. It has significance for studying the biological properties of nanohorns.[12,13] Aqueous dispersions of modified nanohorns obtained without the use of surfactants do not cause the death of primary phagocytic cells.[14] It indicates that after penetration into the cells, the carbon nanoparticles do not exhibit negative effects, at least for several days. Many researchers, working with CNHs, consider that functionalized nanohorns are not toxic and can be successfully used as carriers of biologically active substances and medicines for targeted delivery to organs and tissues of living organisms.[8,10]

The interaction of the "needles" of the nanohorns aggregates with the surface of cell membranes can lead to destruction of the outer membranes bilayer. This may be the main mechanism of nanohorns cytotoxicity[10,15]

CONTACT L. V. Ivanov ivleon@ukr.net Chuiko Institute of Surface Chemistry, NAS of Ukraine, 17 General Naumov Str., 03164 Kiev, Ukraine.

The method of spin probes was already shown to be useful to solve similar problems.[16,17] It can be used to estimate the disorder parameter of phospholipids as well as to evidence an increase in the polarity of the microenvironment of the probe in the outer lipid layer of membranes when they are damaged, using electron paramagnetic resonance (EPR) spectra of paramagnetic labels (stable nitroxide radicals).

The purpose of this paper is to describe the influence of the features of initial and treated CNHs by HNO_3(3M) acid on the microviscosity of the erythrocyte membranes in rats, as well as the change in the polarity and orientation (disorder) of the phospholipids of their outer layer by the method of spin probes. It was evaluated the influence of CNHs on the viscosity of the surface water-protein matrix of blood plasma, primarily on serum albumin (SA) and the interaction features of paramagnetic models of drugs with nanohorns, as potential means of their targeted delivery.

2. Materials and methods

2.1. Synthesis of CNHs

CNHs were synthesized by the electric arc discharge synthesis on an apparatus described earlier.[18,19] The apparatus consists of a water-cooled reaction chamber made of stainless steel with a volume of ~150 L with changeable graphite electrodes moved by a manipulator; it is equipped with a vacuum system and gas regulation and is operated with DC power. During the simultaneous evaporation of seven graphite electrodes with a diameter of 6 mm in the electric arc under the standard synthesis conditions (He pressure of $\sim 10^4$ Pa, current of ~1200 A) carbon nanomaterials are formed on cold walls of the chamber (inCNH).

Carbon nanomaterials in general are poorly soluble in most organic and aqueous solvents. Therefore, to study the properties of CNHs, their surface was treated by nitric acid solution (3 M) at 70 °C for 1 h.[13] After treatment in acid, the sample was washed to neutral pH and dried in a muffle furnace at 100 °C for 10 h (oxCNH).

The probe is a stable nitroxide radical based on palmitic acid (Figure 1). It contains a quaternary ammonium fragment which can be considered as an ionic surfactant compatible with both hydrophobic and hydrophilic media. The lipophilic alkyl fragment of the probe allows it to penetrate into the lipophilic layer of erythrocyte membranes. From the EPR spectra of the probe, the correlation time of Brownian rotational diffusion of the probe in membrane cells and hydrophobic cavities of plasma proteins was evaluated.[20,21] The probe was added to a suspension of erythrocytes or blood plasma from a concentrated solution in DMSO or methanol. The final concentration of the solvent in the suspension of samples was in the range 0.5–1 vol.%.

The preparation procedure of erythrocyte mass and plasma from rat blood was described earlier.[20] The erythrocytic mass and plasma obtained after centrifugation were diluted 2-fold with saline buffer. The erythrocyte concentration was about 9×10^6/mm^3.The SA in dilute plasma was at 30 ± 5 mg/mL.[21,22] Selection and work with animals,

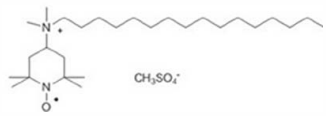

Figure 1. Structure of used spin probe.

statistical processing of the experimental results was carried out as described earlier.[20]

2.2. Characterization

The structure of CNHs was studied using transmission electron microscopy (TEM) with a Jeol 2010 microscope with a lattice resolution of 1.4 Å and point resolution of 1.8 Å as well as by Raman Spectroscopy with Triplemate (Spex) using Ar + laser 488 nm.

Identification of functional groups at the surface of carbon nanostructures was investigated by infrared spectroscopy on IR Fourier spectrometer VERTEX 80.

XPS spectra were measured at the Berlin Elektronenspeicherring für Synchrotronstrahlung (BESSYII) using the Russian-German beamline of monochromatized radiation and the MUSTANG experimental station. The XPS spectra were recorded with a VG CLAM-4 hemispherical analyzer. The photon excitation energy was 800 eV.

Prior to the experiment, the aqueous suspension of nanohorns was sonicated for 30 min by Ultrasonic Cleaner (100 W, 40 kHz). The final concentration of the initial and treated by dilute nitric acid CNHs in the aqueous suspension of erythrocytes or plasma was about 100 μg/mL.

The EPR spectra of the paramagnetic probes in the suspension were recorded at 24 °C using the ESR Spectrometer CMS8400 radio spectrometer. The magnitude of the magnetic field was 2 mT. Microviscosity of erythrocyte membranes was evaluated on the basis of processing the intensity and width of the lines of the EPR spectra of stable nitroxide radicals, spin probes interacting with the external environment (lipid bilayer of erythrocyte membranes, hydrophobic pockets of SA, water).[20,21] The following formula 1 was used to calculate the correlation time of the Brownian rotational diffusion of the probe (τ_c):

$$t_{c(+1/\ 1)} = 6.65 \times 10^{\ 10} C \Delta H_{+1} [(h_{+1}/h_{-1})^{1/2} - 1], \qquad (1)$$

where ΔH_{+1} is the width of the component with the magnetic quantum number of the 14N nucleus ($M = +1$), $h_{+1}, h_{\ 1}$ is the intensity of the components of the EPR spectrum with the magnetic quantum number of the ^{14}N nucleus ($M = +1, -1$).

To estimate the erythrocyte membranes structure, the anisotropy parameter of the EPR spectra (ε) was used. This parameter was determined by the following formula (2)[16,17]:

$$\varepsilon = \left[(h_0/h_{+1})^{1/2} - 1)\right] \Big/ \left[(h_0/h_{\ 1})^{1/2} - 1)\right] \qquad (2)$$

where h_0 is the intensity of the components of the EPR spectrum with the magnetic quantum number of the ^{14}N nucleus ($M = 0$).

All recorded EPR spectra were processed with a computer. A_{iso} parameters, h_0, h_{+1}, $h_{\ 1}$, the time of correlation

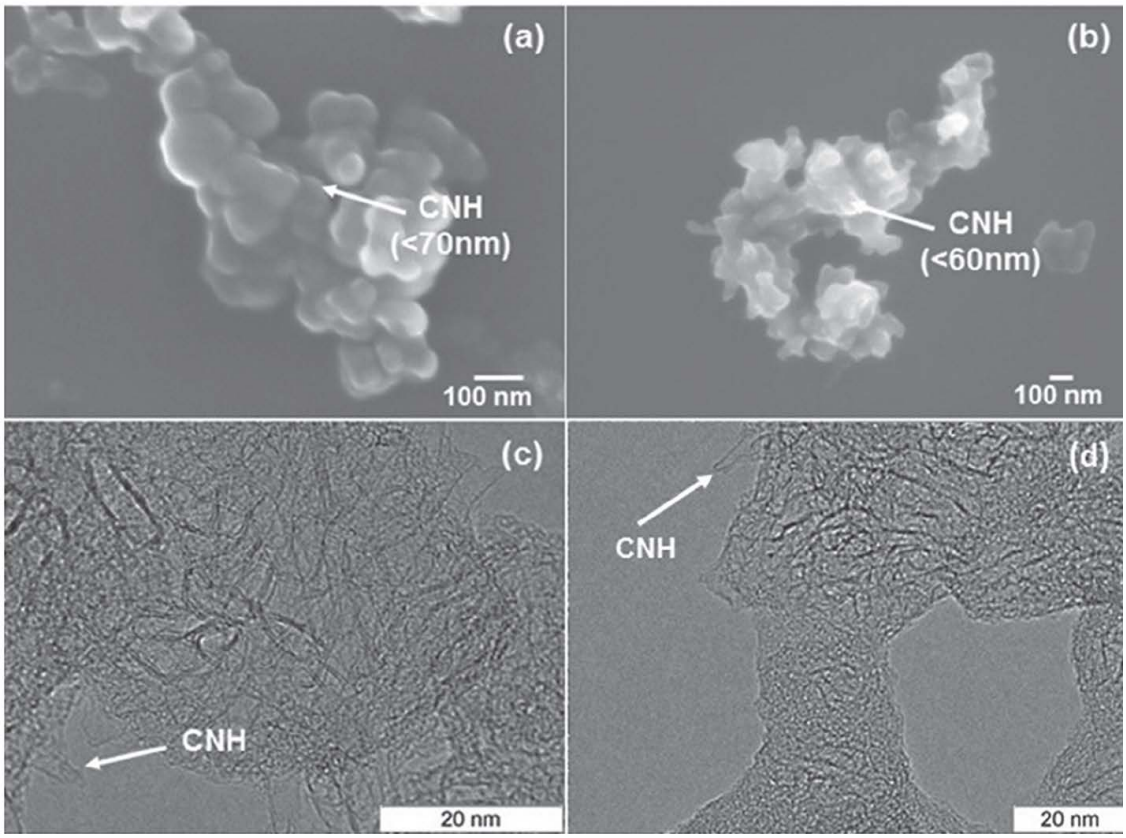

Figure 2. Nanohorns SEM images of (a) initial (inCNH) and (b) treated CNH by HNO_3(3M) (oxCNH); TEM images (c) initial (inCNH) and (d) treated CNH by HNO_3(3M) (oxCNH).

of the rotational diffusion of the probe were automatically measured and calculated.

3. Results and discussion

The morphology of initial and modified CNHs was investigated using SEM and TEM (Figure 2). According to the SEM images, CNHs are agglomerated particles. The average diameter of such particles for inCNH is 70 nm (Figure 2a). After treatment by HNO_3(3M) the nanoparticle size decreased (Figure 2b). The average oxCNH size was 60 nm. TEM images show that CNHs are horn-like nanostructures agglomerated into nanoparticles. The angle of the top of the nanohorns varies from 14° to 17°.

Raman spectra of initial and treated by dilute nitric acid nanohorns are characterized by mainly two modes, D (1350 cm^{-1}) and G (1580 cm^{-1}). The G mode corresponds to tangential atomic vibrations of the graphite lattice (not presented here).[20] The D mode indicates defect carbon states in the graphite mesh.[23,24] The I(D)/I(G) ratio measured for the determination of sample defectiveness was 1.1 and 1.2 for inCNH and oxCNH, respectively. A slight increase in the ratio of integral intensities may be due to decrease in the size of nanoparticle agglomerates. This fact is supported by the SEM data presented above.

The functional groups at CNH surface were identified by infrared spectroscopy (Figure 3a). A broad band at 3400 cm^{-1} is attributed to the presence of O-H vibrations of hydroxyl groups and adsorbed water in the samples. Absorption bands at 1720 cm^{-1} and 1560 cm^{-1} correspond to C=O vibrations of carbonyl groups and the graphite lattice (C=C), respectively. The band at 1030 cm^{-1} is assigned to C–O vibrations of carboxyl groups on the surface of nanohorns.[25] Another band at 1170 cm^{-1} can be attributed to hydroxyl groups.[26] It is seen that after treatment by HNO_3(3M) the band intensity decreases from the spectra. This can indicate a decrease in the oxygen concentration in the sample. This change can be caused by that during treatment by dilute nitric acid the carboxyl groups (COOH) are formed first, and on heating decarboxylation occurs with the release of carbon dioxide. This is confirmed by the XPS O1s spectra shown in Figure 3b. The XPS O1s spectra were fitted by three components. The peak at 532.5 eV is assigned to C=O groups. The peaks at 531.1 eV and 534.6 eV are assigned to COOH and C–OH or C–O–C groups, respectively.[27–29] After treatment in HNO_3(3M) the COOH-component decreases. The oxygen atomic ratio calculated from the peak areas in the survey spectrum shows that its magnitude decreased from 7.4 at. % to 5.3 at.% after treatment by HNO_3(3M) (not represented).

EPR spectra were recorded in a field of 2 mT. The arrow indicates the direction of the sweep of the magnetic field of the radio spectrometer. The EPR spectrum of the spin probe can be described as an ionic surfactant, compatible with both a lyophilic and a lyophobic medium due to the presence of the quaternary nitrogen. In aqueous solutions, probe forms micelles, reminiscent of the structure of the liposome membrane of cells of living organisms. The EPR spectra of

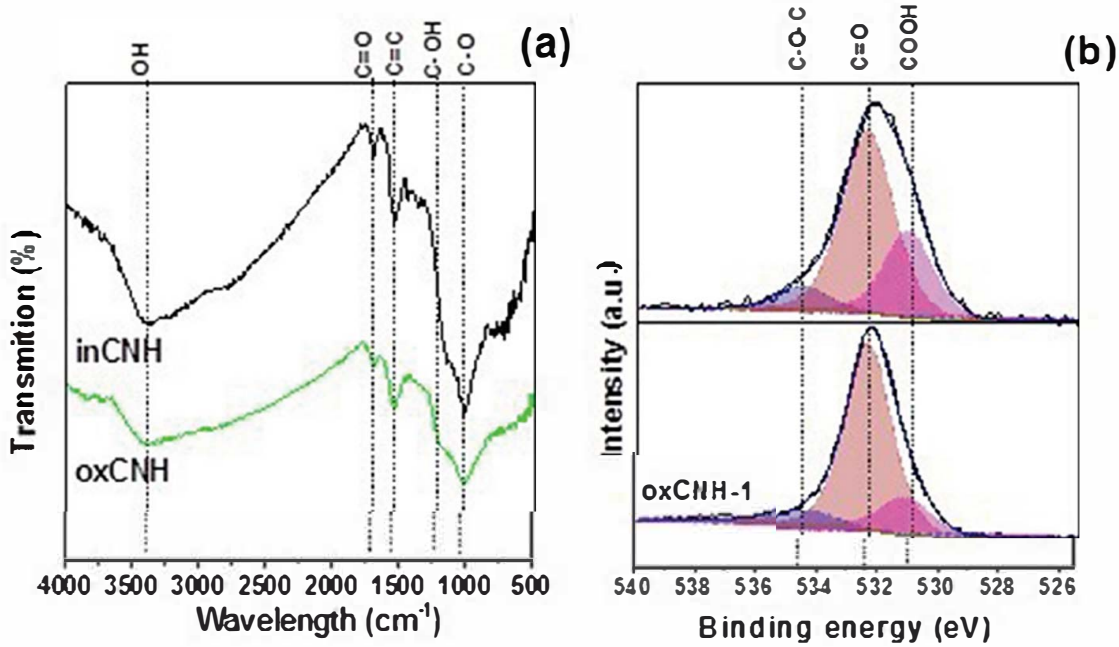

Figure 3. (a) FT IR and (b) XPS O1s spectra and of CNH before (inCNH) and after modification by treatment by nitric acid (oxCNH).

the probe presents a clear triplet, indicating the absence or loss of exchange interactions between nitroxide fragments (Figure 4). The deviations from the ideal triplet 1:1:1 (broadening of the lines, growth of the line half-width, change in the line intensity ratio (h_0, h_{+1}, h_{-1}), and shift of the g-factor) detected in the spectra indicate a significant interaction of the paramagnetic nitroxyl fragment with the components of the medium. From the EPR spectra, the correlation time (τ_c) of the Brownian rotating diffusion probe (formula 1) and the anisotropy parameter (ε) (formula 2) were calculated for different incubation times of nanohorns with a probe (t). A slow progressive decrease in the correlation time of τ is observed and the parameter of the anisotropy (ε) of the spectra increases significantly, when the micelles of the probe are incubated with the nanohorns (Table 1). This means that the nanohorns determine the anisotropy of the Brownian rotational diffusion of the probe in the micelles.[16] The EPR spectra theory[9] relates the experimental parameter ε to the anisotropy of the free radical rotation (d) equal to the ratio of the principal diffusion tensors $D_{II}/D_{\perp}$. A strong increase in ε indicates a significant increase in the anisotropy of the rotation of the probe d in the micelles under the action of nanohorns. Apparently, the interaction of long alkyl "tails" of the probe with cone-shaped "needles" of CNHs aggregates takes place, resulting in the orientation of the probes along the nanohorns, thus increasing the anisotropy of the probe rotation (anisotropy of the EPR spectra).

The EPR spectra of the probe in the blood plasma of rats in the presence of CNHs are quite informative about the effect of nanohorns on protein components. Only SA has three hydrophobic cavities on the surface of the globule from all plasma proteins, which effectively bind various endogenous hydrophobic substrates and transfer them to the blood.[24] The binding effects of labeled fatty acids with SA and the corresponding EPR spectra are well described in the

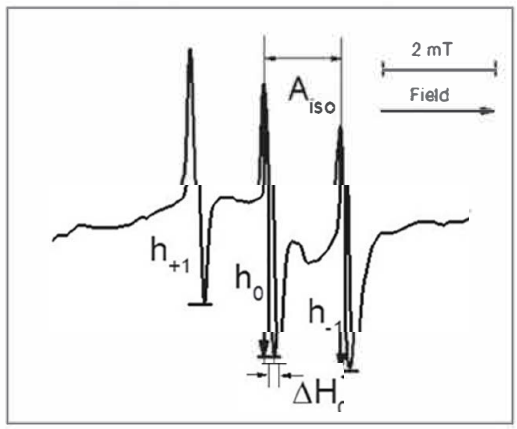

Figure 4. EPR spectrum of the probe in physiological solution 24 h after the introduction of nanohorns.

literature.[20,30–33] Fibrinogen and a number of plasma apolipoproteins also have hydrophobic cavities, but their sorption capacity for hydrophobic substances is lower compared to SA.[20,32–34] Therefore, the addition of probes based on palmitic acid in the plasma guarantees their effective binding with the basic hydrophobic cavity on the surface of the SA. The results of the action of nanohorns on the protein part of the plasma should be associated with the macromolecules of albumin.

Figure 5 shows the EPR spectra of the probe in plasma (hydrophobic cavities of the SA macromolecules) before and 4 h after the addition of initial and treated by dilute nitric acid CNHs to the system.

Despite the qualitatively similar character of the spectra shown in Figure 5, the addition of CNHs changes the parameters of EPR spectra. The data are shown in Table 2. To estimate the polarity of the nitroxyl fragment's microenvironment of spin probes in the membrane, the isotropic hyperfine structure constant was measured (A_{iso}). A_{iso} is

Table 1. Influence of the CNH suspension on the parameters of the EPR spectra of the probe in saline.

Probe environment		t, hour	A_{iso}, Gs	Correlation time $\tau_{c+1} \times 10^9$	$\tau_{c\ 1} \times 10^9$	$\tau_{c+1/\ 1} \times 10^9$	ε
Saline	Without CNH		17.1 ± 0.1	0.058 ± 0.002	0.053 ± 0.002	0.118 ± 0.005	0.48 ± 0.03
	inCNH	1	17.1 ± 0.1	0.035 ± 0.001	0.044 ± 0.002	0.102 ± 0.004	0.64 ± 0.03
		4	17.1 ± 0.1	0.064 ± 0.002	0.043 ± 0.002	0.097 ± 0.004	0.32 ± 0.03
		24	17.0 ± 0.1	0.003 ± 0.0001	0.026 ± 0.001	0.061 ± 0.002	1.05 ± 0.03

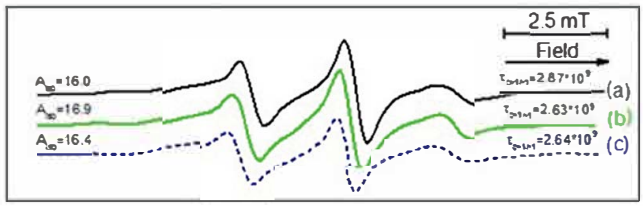

Figure 5. EPR spectra of probe (2) in plasma: (1) in the plasma, (2) 4 h after introduction of inCNH, (3) 4 h after introduction of oxCNH.

Table 2. Influence of the CNH suspension on the parameters of the EPR spectra of the probe in plasma.

Probe environment		t, hour	A_{iso}, Gs	Correlation time $\tau_{c+1} \times 10^9$	$\tau_{c\ 1} \times 10^9$	$\tau_{c+1/\ 1} \times 10^9$	ε
Plasma	inCNH	0	15.9 ± 0.25	1.78 ± 0.09	1.03 ± 0.05	2.87 ± 0.14	0.21 ± 0.03
		0.17	16.0 ± 0.25	1.72 ± 0.08	1.02 ± 0.05	2.78 ± 0.14	0.22 ± 0.03
		1	16.1 ± 0.25	1.65 ± 0.08	1.01 ± 0.05	2.63 ± 0.13	0.21 ± 0.03
		4	16.9 ± 0.25	1.66 ± 0.08	0.94 ± 0.05	2.63 ± 0.13	0.21 ± 0.03
	oxCNH	0.17	16.0 ± 0.25	1.75 ± 0.08	1.04 ± 0.05	2.80 ± 0.14	0.21 ± 0.03
		1	16.4 ± 0.25	1.75 ± 0.08	1.06 ± 0.05	2.79 ± 0.14	0.21 ± 0.03
		4	16.4 ± 0.25	1.65 ± 0.08	1.00 ± 0.05	2.64 ± 0.13	0.21 ± 0.03

distance in gauss between the central (h_0) and high-field ($h_{\ 1}$) components of the EPR spectra (Figure 4).

Thus, the value of the parameter $A_{iso} = 16.0$ Gs for probe in the hydrophobic pocket SA (Figure 5a) indicates the localization of the probe on the surface of the protein globule (for the probe in water $A_{iso} = 17.2$ Gs). Incubation of proteins with a suspension of initial CNHs for 4 h leads to an increase from 16.0 to 16.9 Gs (Figure 5b), due to the interaction between CNHs and the globule SA, increasing the accessibility of the probe to water or weakening the connection of the probe (2) with the hydrophobic pocket of the protein. In this case, the anisotropy parameter ε of the spectrum does not change, because the connection with the hydrophobic SA cavity is preserved. Also, Table 1 data show that incubation of SA with nanohorns leads to a slight decrease in the correlation time ($\tau_{c+1/\ 1}$), which is most sensitive to changes in probe mobility in the medium. The interaction (sorption) of SA macromolecules with the surface of CNHs aggregates is accompanied by numerous contacts with cone-shaped "needles" of single-walled nanohorns with the water-protein SA matrix. It leads to its loosening and weakening of the probe connection with the hydrophobic cavities of the protein.

When treated CNHs are added to the "plasma-probe" system, the value of A_{iso} was 16.4 G after 4 h of incubation (Figure 5c). The polarity of the microenvironment of the probe in the region of the hydrophobic cavity of the protein did not change (see Table 1). The correlation time $\tau_{c+1/\ 1}$ of the probe tends to insignificantly decrease compared to the initial system before the injection of the nanohorns. Thus, it can be concluded that the effect of treated CNHs on the structure of plasma proteins is somewhat milder compared to the initial hydrophobic nanohorns.

The EPR spectrum of the probe in the erythrocyte slurry after 4 h of incubation (Figure 6) exhibits a strongly distorted triplet, which indicates a considerable inhibition of the free rotation of the probe when it is localized in the lipid environment in the membrane.[16,17] The presence of CNHs in the system affects the parameters of the EPR spectra, and this effect can be seen in the dynamics. Figure 7 shows the EPR spectra of the probe in a suspension of erythrocytes with the injection of initial and treated CNHs after 10 min and 1 h. The calculated data on the parameters of the spectra are gathered in Table 1.

Thus, the incubation of erythrocytes with CNHs already after 10 min slightly increases A_{iso} from 14.3 to 14.5 Gs and greatly increases all three parameters of the correlation time of the probe in erythrocyte membranes (the microviscosity of the membranes increases) (Table 3). After 1 h of incubation, A_{iso} increased to 16.1 Gs, evidencing an increase in polarity in the region of the upper layers of membranes and an even greater increase in their microviscosity. According to our estimates, the increase in microviscosity of erythrocyte membranes under the action of CNHs is more than 60%. The special geometry and sufficiently developed surface of CNH nanoparticles, as in the case of CNTs,[24,25] facilitate their binding to the surface of membranes of erythrocytes. This leads to a sharp inhibition (retardation) of the conformational mobility of phospholipids and a decrease in the lateral diffusion of phospholipids along the surface of the

membranes. The effect of nanostructures on the disordering of membrane phospholipids is also indicated by the decrease in the anisotropy parameter ε from 0.23 to 0.19.

The injection of oxCNH into the erythrocyte probe system causes a sharp increase in the microviscosity of membranes. All three correlation time parameters increase, and the spectrum anisotropy parameter decreases to 0.16. This indicates a marked change in the orientation of phospholipids (disordering) as a result of the binding of oxCNHs with the cells. After 1 h incubation, a certain relaxation of the membrane state is observed. The microviscosity values remain high, but 10–15% lower than immediately after the introduction of treated nanohorns into erythrocytes. The parameter ε also relaxes to 0.19. In this case, the adaptive mechanisms of the cell are included after some stress caused by the introduction of treated CNH into the red blood cells. Conformational changes in the main protein of erythrocyte membranes can be attributed to these factors, which ensure the strength of the membrane structure, partial restoration of the initial orientation of phospholipids in the membrane, etc. Also, after 1 h incubation of cells with oxCNHs, A_{iso} increased from 14.3 to 15.6 Gs. This may be due to an increase in polarity in the region of the nitroxide probe head, which is due to the introduction of carbon nanoparticles deep into the membrane. The increase in microviscosity of erythrocyte membranes, estimated by us in terms of parameters $\tau_{c+1/\ 1}$, $\tau_{c\ 1}$ and τ_{c+1} is 52, 79 and 60%, respectively. The relaxation effect of the erythrocyte membrane after the introduction of oxCNH has been recorded on nanoparticles of this type, which possess less cytotoxicity (compared to the initial nanohorns).

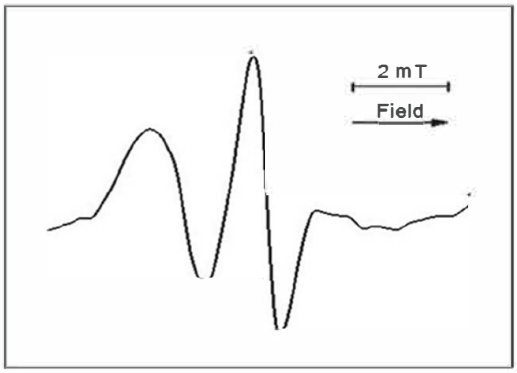

Figure 6. EPR spectrum of probe in the erythrocyte suspension after 4 h incubation of the CNH suspension.

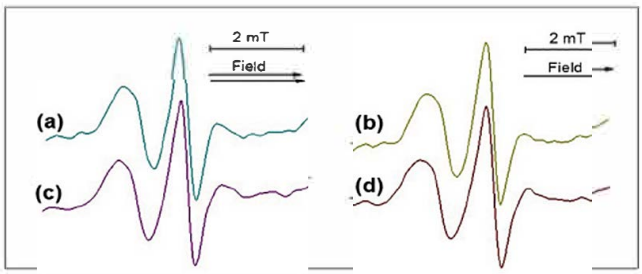

Figure 7. EPR spectra of the probe in the erythrocyte suspension after10 min (a, b) and 1 h (c, d) after introduction of the inCNH (a, c) and oxCHN (b, d).

4. Conclusion

The study of the effect of nanohorns on the structure of the membrane of erythrocytes using the spin probe method revealed a number of new structural changes which were not observed in similar earlier studies.[20,32,33] Interaction between CNHs and the erythrocyte membrane quickly led to a disorder in the phospholipids of the membrane surface with a simultaneous sharp increase in the polarity of the surface lipid layer of the erythrocytes membranes (Figure 8). The increase in the polarity of the lipid layer of erythrocytes membranes and the disorder of phospholipids on the surface of membranes in the presence of CNHs can be explained by the partial destruction of the outer layer of membranes due to their interaction with the nanohorns. Firstly, this is due to the peculiarities of the needle structure of the CNHs. Perhaps, this is the main mechanism of the cytotoxic effect of nanohorns. By comparison with earlier data obtained with CNTs, the cytotoxicity of the initial and treated CNHs can be ranked between the low cytotoxicity of oxidized graphene and cytotoxic nanotubes capable of significantly increasing the microviscosity of erythrocytes membranes and breaking their integrity. Due to low their toxicity, special geometry and high specific surface area, CNHs may be considered as promising carriers of biological substances

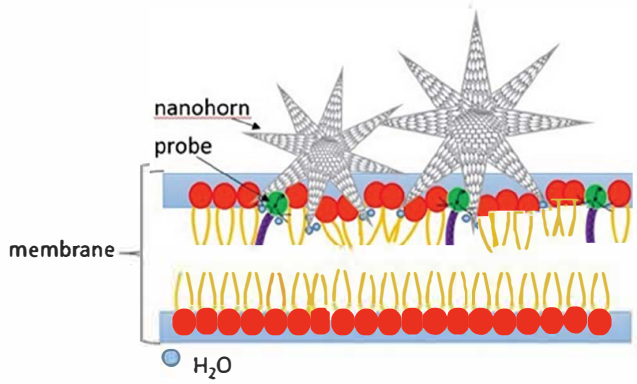

Figure 8. Schematic representation of the nanohorn fragment interaction (needle like nanotubes) with a cell membrane.

Table 3. Influence of the CNH suspension on the parameters of the EPR spectra of the probe in erythrocytic mass from the blood of rats.

Probe environment		t, hour	A_{iso}, Gs	Correlation time $\tau_{c+1} \times 10^9$	$\tau_{c\ 1} \times 10^9$	$\tau_{c+1/\ 1} \times 10^9$	ε
Erythrocyte mass	inCNH	0	14.3 ± 0.25	5.41. ± 0.43	1.86. ± 0.15	9.41. ± 0.75	0.23 ± 0.03
		0.17	14.5 ± 0.25	7.93 ± 0.63	2.80 ± 0.22	13.5 ± 1.08	0.19 ± 0.03
		1	16.1 ± 0.25	8.87 ± 0.71	2.76 ± 0.22	15.26 ± 1.22	0.19 ± 0.03
	oxCNH	0.17	14.3 ± 0.25	8.63 ± 0.7	3.33 ± 0.26	14.3 ± 1.14	0.16 ± 0.03
		1	15.6 ± 0.25	8.31 ± 0.66	2.96 ± 0.24	13.6 ± 1.08	0.19 ± 0.03

and medicines for targeted delivery to the membranes of cells of living organisms.

Funding

The work in part concerning NIIC SB RAS was partially supported by the Basic Research Program of the SB RAS (V.45.1.1).

ORCID

N. T. Kartel http://orcid.org/0000 0002 9431 5921
L. V. Ivanov http://orcid.org/0000 0002 4235 2982
E. Flahaut http://orcid.org/0000 0001 8344 6902
O. A. Gurova http://orcid.org/0000 0002 6531 7709
A. V. Okotrub http://orcid.org/0000 0001 9607 911X

References

[1] Miyawaki, J.; Yudasaka, M.; Azami, T.; Kubo, Y.; Iijima, S. Toxicity of Single Walled Carbon Nanohorns. *ACS Nano* **2008**, *2*, 213 226. DOI: 10.1021/nn700185t.

[2] Maiti, D.; Tong, X.; Mou, X.; Yang, K. Carbon Based Nanomaterials for Biomedical Applications: A Recent Study. *Front. Pharmacol.* **2019**, *9*, 1401. DOI: 10.3389/fphar.2018.01401.

[3] Prylutska, S. V.; Grebinyk, A. G.; Lynchak, O. V.; Byelinska, I. V.; Cherepanov, V. V.; Tauscher, E.; Matyshevska, O. P.; Prylutskyy, Y. I.; Rybalchenko, V. K.; Ritter, U.; et al. In Vitro and in Vivo Toxicity of Pristine C 60 Fullerene Aqueous Colloid Solution. *Fuller. Nanotub. Carbon Nanostruct.* **2019**, *27*, 715 728. DOI: 10.1080/1536383X.2019.1634055.

[4] Popov, V. A.; Tyunin, M. A.; Zaitseva, O. B.; Karaev, R. H.; Sirotinkin, N. V.; Dumpis, M. A.; Piotrovsky, L. B. C60/PVP Complex No Toxicity after Introperitoneal Injection to Rats. *Fuller. Nanotub. Carbon Nanostruct.* **2008**, *16*, 693 697. DOI: 10.1080/15363830802317130.

[5] Moussa, F.; Trivin, F.; Céolin, R.; Hadchouel, M.; Sizaret, P. Y.; Greugny, V.; Fabre, C.; Rassat, A.; Szwarc, H. Early Effects of C 60 Administration in Swiss Mice: A Preliminary Account for in Vivo C 60 Toxicity. *Fuller. Sci. Technol.* **1996**, *4*, 21 29. DOI: 10.1080/10641229608001534.

[6] Tomchuk, A. A.; Shershakova, N. N.; Andreev, S. M.; Turetskiy, E. A.; Ivankov, O. I.; Kyzyma, O. A.; Tomchuk, O. V.; and Avdeev, M. V. C. C60 Arginine Aqueous Solutions: In Vitro Toxicity and Structural Study. *Fuller. Nanotub. Carbon Nanostruct.* **2020**, *28*, 245 249. DOI: 10.1080/1536383X.2019.1697242.

[7] Francis, A. P.; Devasena, T. Toxicity of Carbon Nanotubes: A Review. *Toxicol. Ind. Health* **2018**, *34*, 200 210. DOI: 10.1177/0748233717747472.

[8] Iijima, S.; Yudasaka, M.; Yamada, R.; Bandow, S.; Suenaga, K.; Kokai, F.; Takahashi, K. Nano Aggregates of Single Walled Graphitic Carbon Nano Horns. *Chem. Phys. Lett.* **1999**, *309*, 165 170. DOI: 10.1016/S0009 2614(99)00642 9.

[9] Murata, K.; Kaneko, K.; Kokai, F.; Takahashi, K.; Yudasaka, M.; Iijima, S. Pore Structure of Single Wall Carbon Nanohorn Aggregates. *Chem. Phys. Lett.* **2000**, *331*, 14 20. DOI: 10.1016/S0009 2614(00)01152 0.

[10] Piotrovskii, L. B.; Melik Ogandzhanyan, R. G. Properties and Biological Potential of Single Walled Carbon Nanohornes. *FARMA* **2011**, *1*, 120 128.

[11] Zhu, S.; Xu, G. Single Walled Carbon Nanohorns and Their Applications. *Nanoscale* **2010**, *2*, 2538. DOI: 10.1039/c0nr00387e.

[12] Murakami, T.; Sawada, H.; Tamura, G.; Yudasaka, M.; Iijima, S.; Tsuchida, K. Water Dispersed Single Wall Carbon Nanohorns as Drug Carriers for Local Cancer Chemotherapy. *Nanomedicine* **2008**, *3*, 453 463. DOI: 10.2217/17435889.3.4.453.

[13] Datsyuk, V.; Kalyva, M.; Papagelis, K.; Parthenios, J.; Tasis, D.; Siokou, A.; Kallitsis, I.; Galiotis, C. Chemical Oxidation of Multiwalled Carbon Nanotubes. *Carbon N.Y.* **2008**, *46*, 833 840. DOI: 10.1016/j.carbon.2008.02.012.

[14] Lacotte, S.; García, A.; Décossas, M.; Al Jamal, W. T.; Li, S.; Kostarelos, K.; Muller, S.; Prato, M.; Dumortier, H.; Bianco, A. Interfacing Functionalized Carbon Nanohorns with Primary Phagocytic Cells. *Adv. Mater.* **2008**, *20*, 2421 2426. DOI: 10.1002/adma.200702753.

[15] Ajima, K.; Yudasaka, M.; Murakami, T.; Maigné, A.; Shiba, K.; Iijima, S. Carbon Nanohorns as Anticancer Drug Carriers. *Mol. Pharmaceutics* **2005**, *2*, 475 480. DOI: 10.1021/mp0500566.

[16] Liechtenstein, G. I. *The Method of Spin Labels in Molecular Biology*; Nauka Moscow, Russia, **1974**.

[17] Berliner, L. J., Eds. *The Method of Spin Labels. Theory and Applications*; Mir, Moscow, Russia, **1979**.

[18] Okotrub, A. V.; Shevtsov, Y. V.; Nasonova, L. I.; Sinyakov, D. E.; Chuvilin, A. L.; Gutakovskii, A. K.; Mazalov, L. N. Synthesis of Monolayer Closed Carbon Particles in an Electric Arc Discharge. *Inorg. Mater.* **1996**, *32*, 974 978.

[19] Gurova, O. A.; Omelyanchuk, L. V.; Dubatolova, T. D.; Antokhin, E. I.; Eliseev, V. S.; Yushina, I. V.; Okotrub, A. V. Synthesis and Modification of Carbon Nanohorns Structure for Hyperthermic Application. *J. Struct. Chem.* **2017**, *58*, 1205 1212. DOI: 10.1134/S0022476617060191.

[20] Kartel, M. T.; Ivanov, L. V.; Lyapunov, O. M.; Nardid, O. A.; Cherkashina, Y.; Shcherbak, E. V.; Gurova, O. A.; O.; Okotrub, A. V. Effect of Carbon Nanoparticles of Different Nature on the Micro Viscosity of Erythrocyte Membranes of Experimental Animals. *Him. Fiz. Tehnol. Poverhni* **2019**, *10*, 312 323. DOI: 10.15407/hftp10.03.312.

[21] Moiseeva, N. N.; Kravchenko, L. P.; Semenchenko, A. A.; Petrenko, A. Y. Effect of Transplantation of Hepatocytes Subjected to Hypothermic Storage on Liver Regeneration in Rats after Partial Hepatectomy. *Probl. Cryobiol.* **2002**, *1*, 24.

[22] Peña Álvarez, M.; Corro, E. d.; Langa, F.; Baonza, V. G.; Taravillo, M. Morphological Changes in Carbon Nanohorns under Stress: A Combined Raman Spectroscopy and TEM Study. *RSC Adv.* **2016**, *6*, 49543 49550. DOI: 10.1039/C5RA27162B.

[23] Dresselhaus, M. S.; Jorio, A.; Saito, R. Characterizing Graphene, Graphite, and Carbon Nanotubes by Raman Spectroscopy. *Annu. Rev. Condens. Matter Phys.* **2010**, *1*, 89 108. DOI: 10.1146/annurev conmatphys 070909 103919.

[24] Misra, A.; Tyagi, P.; Rai, P.; Misra, D. S. FTIR Spectroscopy of Multiwalled Carbon Nanotubes: A Simple Approach to Study the Nitrogen Doping. *J. Nanosci. Nanotechnol.* **2007**, *7*, 1820 1823. DOI: 10.1166/jnn.2007.723.

[25] Shlyakhova, E. V.; Bulusheva, L. G.; Kanygin, M. A.; Plyusnin, P. E.; Kovalenko, K. A.; Senkovskiy, B. V.; Okotrub, A. V. Synthesis of Nitrogen Containing Porous Carbon Using Calcium Oxide Nanoparticles. *Phys. Status Solidi B* **2014**, *251*, 2607 2612. DOI: 10.1002/pssb.201451228.

[26] Wepasnick, K. A.; Smith, B. A.; Bitter, J. L.; Howard Fairbrother, D. Chemical and Structural Characterization of Carbon Nanotube Surfaces. *Anal. Bioanal. Chem.* **2010**, *396*, 1003 1014. DOI: 10.1007/s00216 009 3332 5.

[27] Bulusheva, L. G.; Okotrub, A. V.; Asanov, I. P.; Fonseca, A.; Nagy, J. B. Comparative Study on the Electronic Structure of Arc Discharge and Catalytic Carbon Nanotubes. *J. Phys. Chem. B* **2001**, *105*, 4853 4859. DOI: 10.1021/jp010056v.

[28] Fedoseeva, Y. V.; Pozdnyakov, G. A.; Okotrub, A. V.; Kanygin, M. A.; Nastaushev, Y. V.; Vilkov, O. Y.; Bulusheva, L. G. Effect of Substrate Temperature on the Structure of Amorphous Oxygenated Hydrocarbon Films Grown with a Pulsed Supersonic Methane Plasma Flow. *Appl. Surf. Sci.* **2016**, *385*, 464 471. DOI: 10.1016/j.apsusc.2016.05.120.

[29] Mazov, I.; Kuznetsov, V. L.; Simonova, I. A.; Stadnichenko, A. I.; Ishchenko, A. V.; Romanenko, A. I.; Tkachev, E. N.;

Anikeeva, O. B. Oxidation Behavior of Multiwall Carbon Nanotubes with Different Diameters and Morphology. *Appl. Surf. Sci.* **2012**, *258*, 6272 6280. DOI: 10.1016/j.apsusc.2012.03.021.

[30] Salvador Morales, C.; Flahaut, E.; Sim, E.; Sloan, J.; Green, M. L. H.; Sim, R. H. Complement Activation and Protein Adsorption by Carbon Nanotubes. *Mol. Immunol.* **2006**, *43*, 193 201. DOI: 10.1016/j.molimm.2005.02.006.

[31] Sergeev, P. V., Ed. *Biochemical Pharmacology*; Higher School, Moscow, Russia, **1982**.

[32] Ivanov, L. V.; Lyapunov, O. M.; Kartel, M. T.; Nardid, OA.; Okotrub, AV.; Kirilyuk, I. A.; Cherkashina Ya. O. Delivery of Spin Probes by Carbon Nanotubes in Erythrocytes and Plasma of Blood. *Surface* **2014**, *6*, 292 304.

[33] Kartel, N. T.; Ivanov, L. V.; Lyapunov, A. N.; Nardid, O. A.; Okotrub, A. V.; Kiril, I. A. Evaluation of the Effect of Carbon Nanotubes on the Microviscosity of Erythrocyte Membranes. *Rep. Natl. Acad. Sci. Ukraine* **2015**, *3*, 114.

[34] Zhdanov, R. I. *Paramagnetic Models of Biologically Active Compounds*. Nauka, Moscow, Russia, **1981**.